



Compact, printed, UWB, fiberglass textile antenna with quadruple band-notched characteristics for WLAN/WiMAX

Ankan Bhattacharya⁽¹⁾, Arnab De⁽²⁾, Bappaditya Roy*⁽³⁾ and Anup K. Bhattacharjee⁽²⁾

⁽¹⁾Dept. of Electronics & Communication Engg., Mallabhum Institute of Technology, Bishnupur, India

⁽²⁾Dept. of Electronics & Communication Engg., National Institute of Technology, Durgapur, India

⁽³⁾School of Electronics Engineering., VIT-AP University, Amaravati, AP, India

bappaditya13@gmail.com

Abstract

Herein, a printed Ultra-Wideband (UWB) monopole antenna possessing quadruple band-notched characteristics has been investigated. A fiberglass textile composite laminate has been used as the substrate material. Complementary Split Ring Resonating Structures have been introduced at the centre of the fractal radiator to pro-create band notches for the 03.5/05.2 GHz WiMAX/WLAN bands. Two ‘C-shaped’ parasitic structures have been placed near both sides of the microstrip feed to generate a notch for 05.5 GHz WiMAX band. Two ‘L-shaped’ slits have been introduced near the edges of the fractional ground plane to produce a notch for the 05.8 GHz WLAN band. The proposed fractal monopole antenna shows UWB response from 02.7 – 11.5 GHz along with quadruple band-notched features. Simulated and measured responses tallied fairly well. The wearable textile antenna proposed here, is a novel contender for UWB communication possessing multiple band-notched features.

1 Introduction

In the last decade Ultra Wideband (UWB) technology has drawn a significant attention of antenna researchers. High transmission speed, wide bandwidth are the key features of UWB transmission systems. The use of UWB technology within the frequency range of 03.1-10.6 GHz was commercialized by Federal Communications Commission (FCC) in the year 2002 [1]. Though UWB technology had been quite popular, the problem arose when frequency interference resulted from other narrow band systems like the 03.5/05.5 GHz WiMAX freq. band and the 05.2/05.8 GHz WLAN freq. band. To bypass the interference effect many UWB antennas with single/multiple band-notched characteristics have been developed. A printed wide-slot UWB antenna has been proposed Gao et al. in [2] with two freq. notches centered at 03.5 GHz and 05.5 GHz respectively. A wideband antenna with a circular patch and freq. band notches centered at 03.5 GHz and 05.5 GHz for filtering WiMAX and WLAN bands has been proposed by Shuai et al. in [3]. A Co-planar Waveguide (CPW) fed antenna with a wide bandwidth and band notches centered at 05.5 GHz WLAN band and 08.0 GHz X-band has been reported by

Li et al. in [4]. An UWB monopole antenna possessing freq. notches for WLAN and WiMAX bands has been proposed by Zhou et al. in [5]. A slotted wideband antenna with band-notches for WiMAX and WLAN bands has been proposed by Samadi et al. in [6]. A planar, UWB, dual band-notched antenna with SRR has been proposed by Li et al. in [7] for upper and lower WLAN frequency bands. However, the number of band notches in the aforesaid antennas is limited to one or two. Few are triple or quad band-notched as in [8-10], but the size/area of the antenna is an issue in every case.

Here, we have designed and investigated a UWB antenna with quadruple band-notched features. A fiberglass composite laminate G-10 has been used as the substrate material. Complementary Split Ring Resonating Structures have been introduced at the centre of the snowflake radiator to create band notches for the 03.5/05.2 GHz WiMAX/WLAN bands. Two ‘C-shaped’ parasitic structures have been placed alongside the feed line to generate a notched band for 05.5 GHz WiMAX band. Two ‘L-shaped’ slits have been introduced near the edges of the slotted ground plane to produce notch for the 05.8 GHz WLAN band. The proposed fractal monopole antenna shows UWB response from 02.7 – 11.5 GHz along with quadruple band-notched features. Antenna responses, both simulated as well as measured, showed a good agreement. The proposed antenna has been compared with notable UWB band-notched antennas in Table 1, based on compactness i.e. size/area and features.

Table 1: comparison of notable band-notched uwb antennas

Ref. No.	Size [mm ²]	Area [mm ²]	BW [GHz]	Notched Bands
[2]	20 × 27	540	2.89 - 11.52	Two
[3]	34 × 26	884	2.80 - 10.70	Two
[4]	21 × 28	588	3.10 - 10.60	Two
[5]	24 × 28	672	2.91 - 11.40	Two
[6]	23 × 28	644	3.10 - 11.00	Two
[7]	24 × 25	600	3.05 - 14.20	Two
[8]	30 × 30	900	3.01 - 12.00	Three
[9]	28 × 32	896	2.90 - 13.40	Three
[10]	20 × 30	600	2.68 - 13.00	Four
Prop	15 × 32	480	2.70 - 11.50	Four

2 Antenna design and simulation

Koch Snowflake Fractal Geometry has been incorporated in the Patch of the proposed radiating structure. H. Koch first introduced this geometry in 1904 [11]. This geometry is generated by an Iterative-Function-System (IFS). It is obtained by a group of overlapping equilateral triangles.

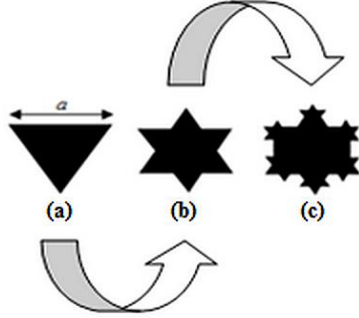


Figure 1. Koch fractal geometry in successive iterations: (a) basic geometry, (b) First iteration, and (c) Second iteration

In Figure 1, the iterative Koch structure has been displayed. After an iterative transform n , there is an increase in the overall geometrical area. If S_n is the area of each iteration n , then overall area of successive iterations can be obtained as,

$$S_{n+1} = S_n + (\sqrt{3}/12) \cdot (4/9)^{n-1} \cdot a^2 \quad (1)$$

where a = length of the side of an equilateral triangle, whose area is equal to

$$S_o = (\sqrt{3}/4) \cdot a^2 \quad (2)$$

The antenna formed by applying the 2nd iterative geometrical stage in CST Microwave Studio environment has been represented in Figure 2. G-10 material, having electrical permittivity (ϵ_r) of 4.8 and loss tangent ($\tan \delta$) of 0.008 has been used as a material for the substrate. G-10 is like a glass fiber and a composite material which consists of a glass filament like continuous cloth and binded by epoxy resin. Few characteristics of G-10 are high durability, less absorption of moisture, high resistance to chemicals and promising electrical characteristics. On the rear side of the antenna there is the Defected Ground Structure (DGS). The feed line width (Fw) should be carefully selected. It is an important parameter which affects the impedance match between the source of current and the radiator. There should be an impedance match between the source element and the load resistance for maximum power to be transferred. The feed line has approximately been matched to 50 Ω following equations (3) and (4).

$$\epsilon_{eff} = \frac{\epsilon_r + 1}{2} + \frac{\epsilon_r - 1}{2} [\sqrt{1 + 12(h/Fw)}]^{-1}, \quad (3)$$

$$Z_o = \frac{120\pi}{\sqrt{\epsilon_{eff}} \left[\frac{Fw}{h} + 1.393 + 0.667 \ln \left(\frac{Fw}{h} + 1.444 \right) \right]}, \quad (4)$$

for $Fw/h \geq 1$. Z_o is known as the characteristic impedance and ϵ_{eff} is the dielectric constant (effective) of substrate [12]. An optimum feed line width F_w of 1.0 mm has been selected to approximately match the 50 Ω input impedance. For the proposed design, substrate dielectric constant, $\epsilon_r = 4.8$ (G-10) and substrate height, $h = 0.75$ mm. As observed from Figure 3, the VSWR is less than 2 starting from 02.7 GHz and continuing till 11.5 GHz.

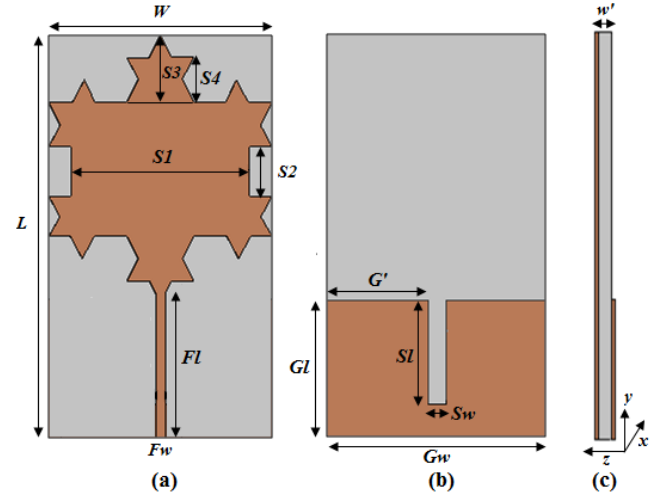


Figure 2. Antenna 1: (a) Front face (b) Rear face (c) Side face.

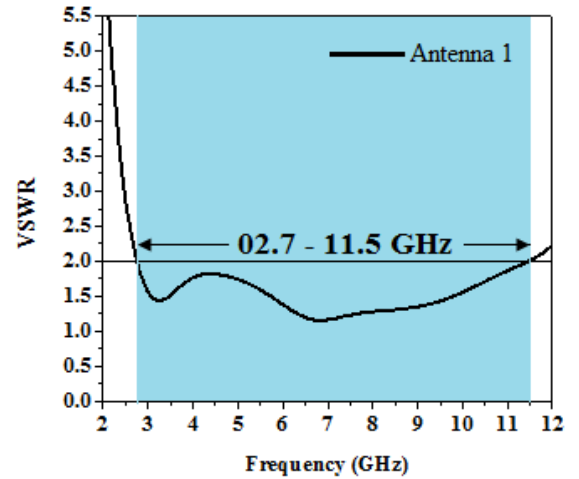


Figure 3. VSWR vs. Frequency response of Antenna 1.

Now, our objective is to create a notch at the 03.3-03.7 GHz WiMAX band. With this motto in mind, we have introduced a Complementary Split Ring Resonating (CSRR) structure at the centre of the radiating element. Equivalent circuit model of CSRR structure has been represented in Figure 4. The CSRR, here, behaves as an L-C resonant circuit. The resonant frequency of the CSRR unit cell can be determined by Inductance, L and Capacitance, C per unit length. The resonant frequency, f_r of the CSRR can be expressed as,

$$f_r = \frac{1}{2\pi\sqrt{L'C'}} \quad (5)$$

where L' and C' are the total inductance and total capacitance of the structure.

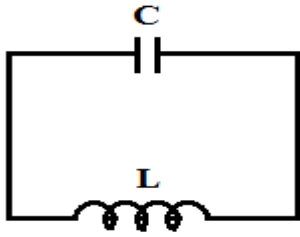


Figure 4. Equivalent circuit of CSRR structure.

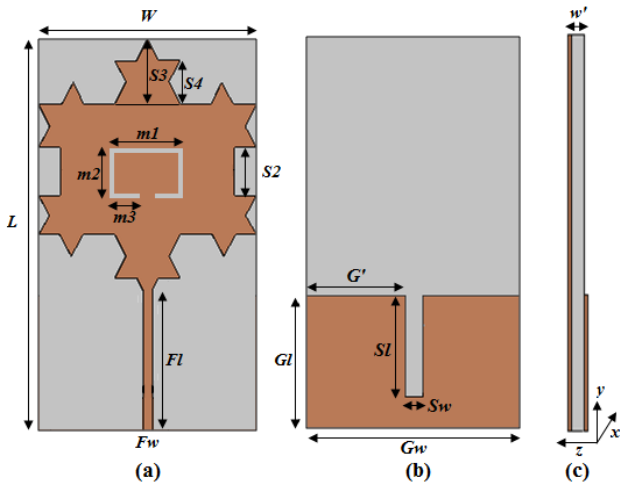


Figure 5. Antenna 2: (a) Front face (b) Rear face (c) Side face.

The structure of the modified antenna i.e. Antenna 2 has been displayed in Figure 5, which consists of a CSRR structure at the centre of the radiator. Figure 6. shows VSWR vs. Frequency response of Antenna 2. By appropriate choice of dimensions of CSRR structure the centre-freq. of the band-notch is finely tuned to 3.5 GHz.

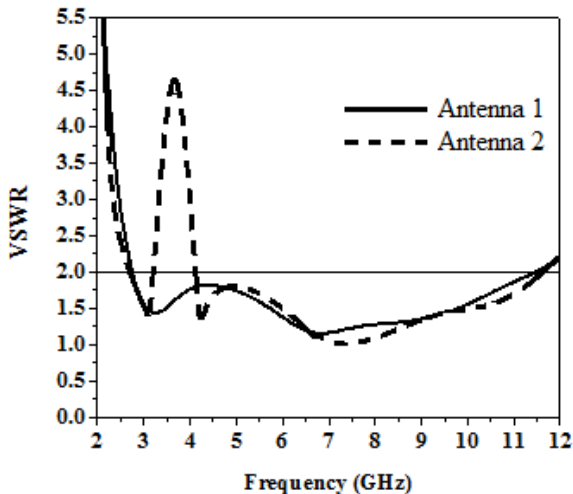


Figure 6. VSWR vs. Frequency response of Antenna 2.

For generating a notch for the 05.19-5.21 GHz WLAN band. For this purpose we have introduced another CSRR structure as displayed in Figure 7 (Antenna 3). By appropriate choice of dimensions we have been successful in generating a notch centred at 05.2 GHz. The VSWR vs. Frequency response of Antenna 3 has been shown in Figure 8. Antenna 3 formed, is a dual band-notched antenna. It may be noted from Figure 8 that there is no significant change or disturbance of the notched band at 03.5 GHz due to the incorporation of the second CSRR structure.

A band-notch feature has been obtained in the 05.25 – 05.75 GHz range for elimination of the interference from the existing WiMAX band centered at 5.5 GHz due to the incorporation of two open-circuited C-shaped stubs at the two sides of the feeding segment.

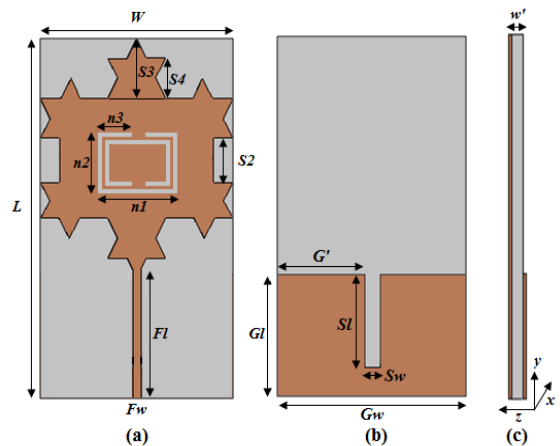


Figure 7. Antenna 3: (a) Front view (b) Rear view (c) Side view.

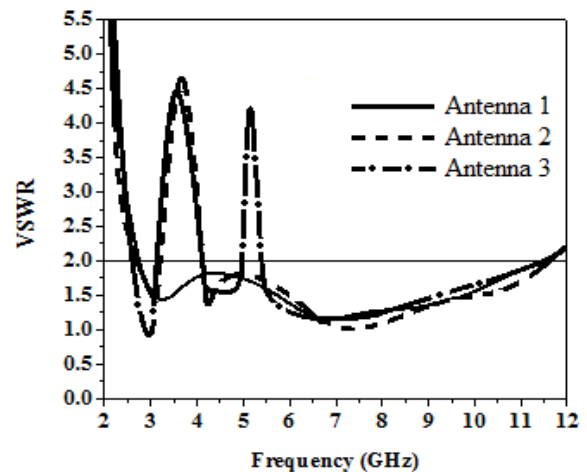


Figure 8. VSWR vs. Frequency response of Antenna 3.

A band-notch feature has been obtained in the 05.25 – 05.75 GHz range for elimination of the interference from the existing WiMAX band centered at 5.5 GHz due to the incorporation of two open-circuited C-shaped stubs at the two sides of the feeding segment.

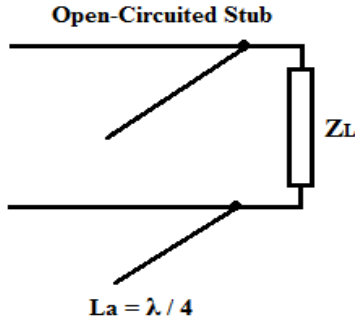


Figure 9. Equivalent model of Open-Circuited Stub.

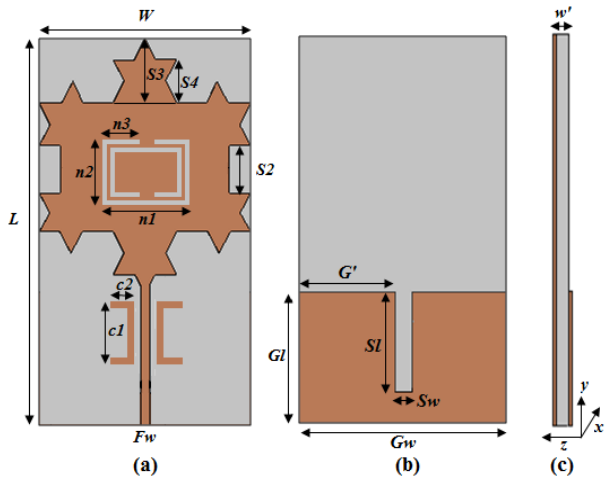


Figure 10. Antenna 4: (a) Front view (b) Rear view (c) Side view.

The equivalent model of open-circuited stub has been represented in Figure 9. The perimeter of the stub, L_a is approximately equal to the quarter of the guide wavelength at the notched frequency point. The wavelength of guide can be expressed as,

$$\lambda = \frac{c}{f_{notch} \sqrt{\epsilon_{eff}}} \quad (6)$$

where c is the light velocity in vacuum, f_{notch} is the centre freq. of the notch band and ϵ_{eff} is the effective relative permittivity of the substrate. The modified antenna (Antenna 4) with open-circuited stubs located at both sides of the feeding segment has been depicted in Figure 10. The VSWR characteristic of Antenna 4 has been depicted in Figure 11.

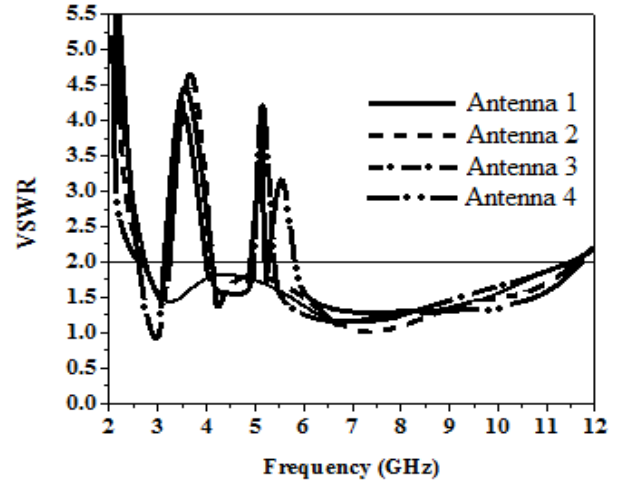


Figure 11. VSWR-Freq. characteristics of Antenna 4.

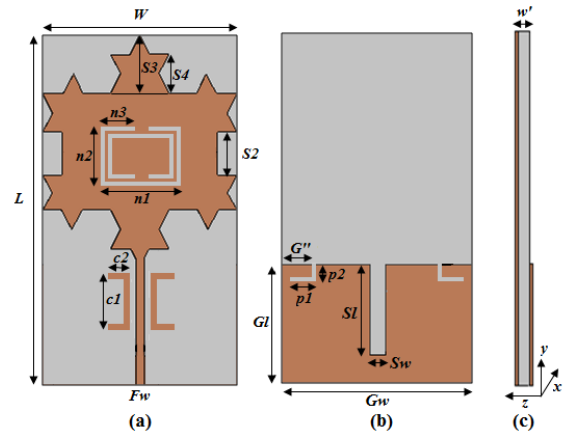


Figure 12. Antenna 5: (a) Front view (b) Rear view (c) Side view.

In order to generate a notch for the 05.795–5.815 GHz WLAN band, we have introduced ‘L-shaped’ slits at the edges of the partial ground plane. The dimensions of the slit are adjusted for obtaining the centre frequency of the notch at 05.8 GHz.

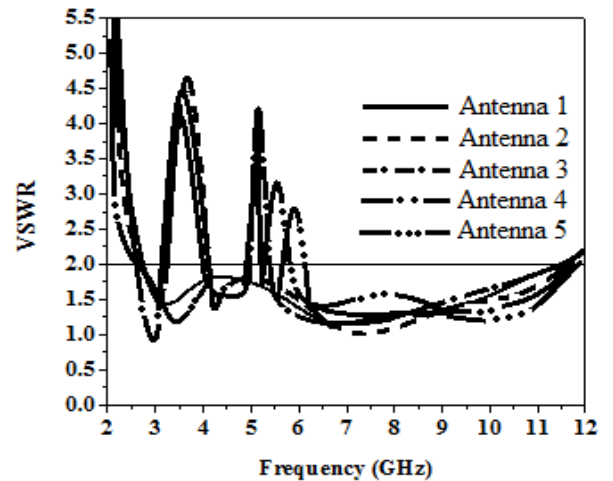


Figure 13. VSWR-Freq. characteristics of Antenna 5.

The proposed antenna structure (Antenna 5), with slits in the ground plane has been depicted in Figure 12. The VSWR vs. Frequency response of Antenna 5 has been shown in Figure 13. Antenna 5 shows a wide frequency response ranging from 02.7 – 11.5 GHz along with four notched-bands centred at 03.5 GHz, 05.2 GHz, 05.5 GHz and 05.8 GHz respectively. The various dimensions of Antenna 1 to Antenna 5 are $W = 15.0$ mm, $L = 32.0$ mm, $Fw = 01.0$ mm, $Fl = 13.0$ mm, $Gw = 15.0$ mm, $Gl = 12.75$ mm, $Sw = 02.0$ mm, $S1 = 07.25$ mm, $p1 = 02.5$ mm, $p2 = 02.0$ mm, $G'' = 03.0$ mm, $S2 = 04.75$ mm, $S3 = 05.0$ mm, $S4 = 03.25$ mm, $n1 = 06.0$ mm, $n2 = 05.25$ mm, $n3 = 03.0$ mm, $c1 = 05.0$ mm, $c2 = 02.0$ mm and $w' = 01.75$ mm.

3 Fabrication, measurement and analysis

The proposed antenna i.e. Antenna 5 has been fabricated in order to compare the simulated values with those obtained from measurement. Figure 14. shows the foremost, rearmost and magnified view of the antenna fabricated with fiberglass substrate.

Figure 15 shows simulated vs. measured frequency response of antenna VSWR. The cause of generation of the band notches can be justified by analyzing the flow of antenna surface current at various frequency point(s). The pattern of distribution of antenna surface at various frequencies have been represented in Figures 16 (a), (b), (c) and (d).

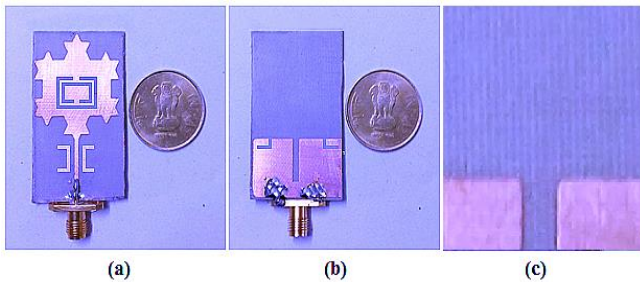


Figure 14. Fabricated prototype: (a) Front face (b) Rear face (c) Magnified view

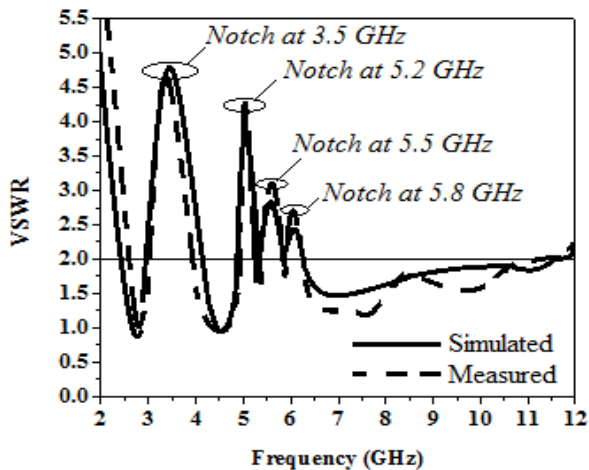


Figure 15. VSWR vs. Frequency response of Antenna 5.

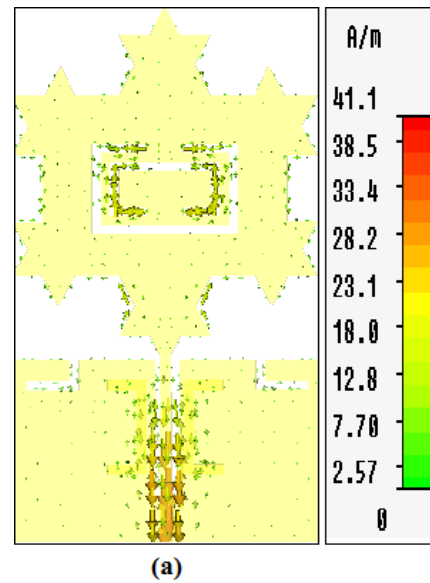


Figure 16 (a). Antenna surface current flow at 03.5 GHz

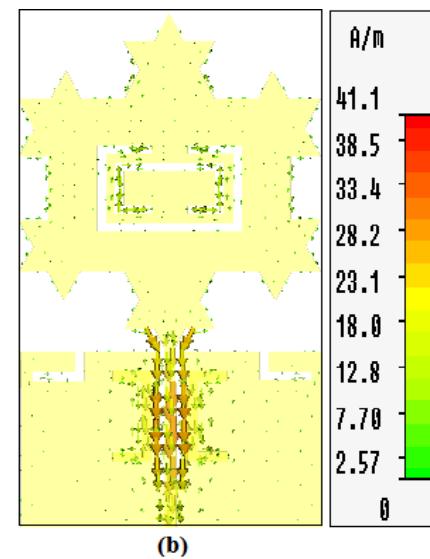


Figure 16 (b). Antenna surface current flow at 05.2 GHz

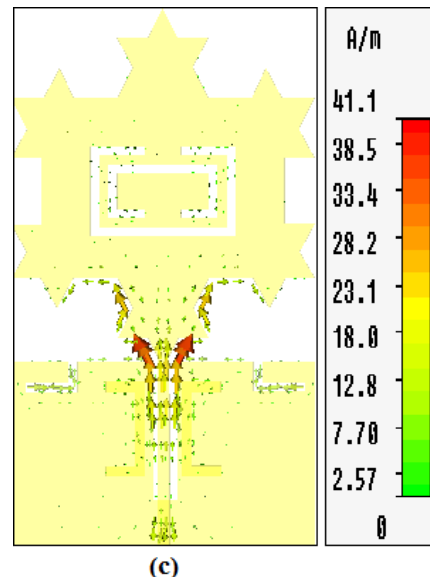


Figure 16 (c). Antenna surface current flow at 05.5 GHz

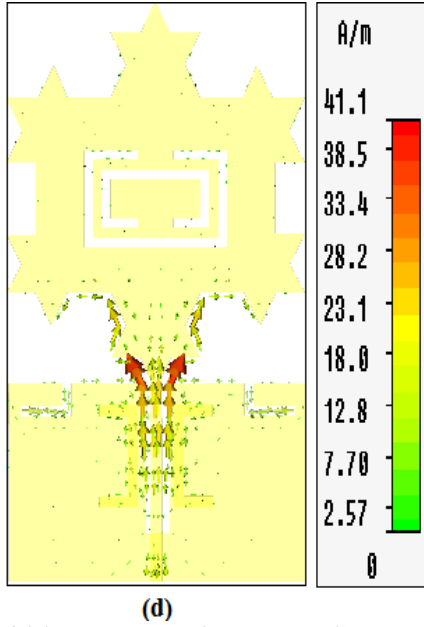


Figure 16 (d). Antenna surface current flow at 05.8 GHz.

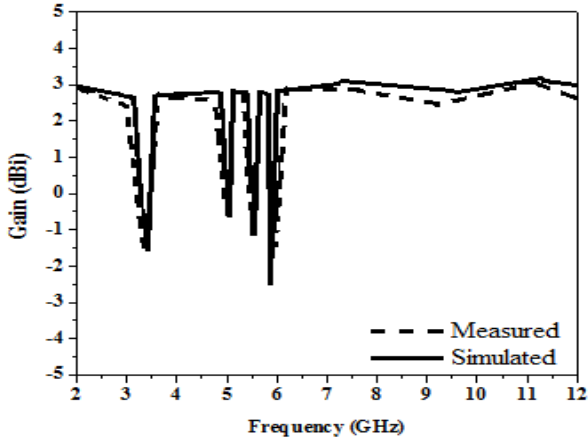


Figure 17. Antenna Gain vs. Frequency.

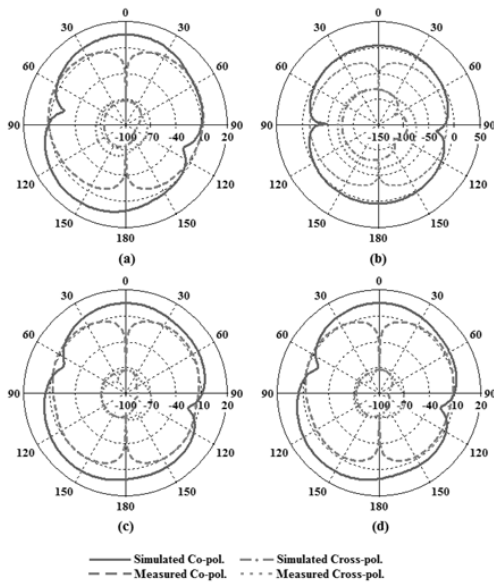


Figure 18. Radiation pattern of proposed antenna: (a) 03.5 GHz, (b) 05.2 GHz, (c) 05.5 GHz, and (d) 05.8 GHz.



Figure 19 (a) and (b) Set-up for measurement of various antenna parameters.

As observed from Figs. 16 (a) and (b), the surface current tends to concentrate near the CSRR structures at 03.5 GHz and 05.2 GHz. Similar things can be observed from Figure 16 (c), where the surface current tends to accumulate near the C-shaped open circuited parasitic stubs at 05.5 GHz. Figure 16 (d) shows that the surface current has accumulated around the open-ended L-shaped slits on the partial ground plane at 05.8 GHz. Therefore, it is clear that the presence of these band-notching structures are responsible for the uneven distribution of antenna surface current and generation of notched bands at various frequencies. Figure 17 shows simulated vs. measured gain in dBi vs. Frequency. It can be observed that there is an abrupt fall in antenna gain at the band-notched frequency point(s). The band-notching structures are responsible for this drastic reduction of gain below the 0 dBi level. Figure 18 shows the simulated and measured Co-Pol. and Cross-Pol. components of the radiation pattern of the antenna proposed. The pattern of radiation is nearly omnidirectional with good isolation between the components of Co-Pol. and Cross-Pol.. Figure 19 (a) and (b) show the set-up for measurement of various antenna parameters. Analysis of the time domain response i.e. the Group Delay factor is very important. The Group Delay of the signal can be formulated as,

$$g\delta = -\Delta\theta/\Delta\varphi \quad (7)$$

where, $\Delta\theta$ and $\Delta\varphi$ are the signal phase deviation and freq. deviation respectively. The change in group delay accounts for the distortion in signal. As noticed from Figure 20, the group delay pattern is similar all through with some ripples ≤ 0.15 ns. The Tx and the Rx had been placed at a gap of $d = 25$ cm. Group delay response of proposed antenna obeys the considerable limits throughout the whole impedance-bandwidth with an exception at the notched-frequency bands. One can observe the presence of undesired oscillations in the antenna time domain analysis. These unwanted fluctuations occur due to the presence of noise.

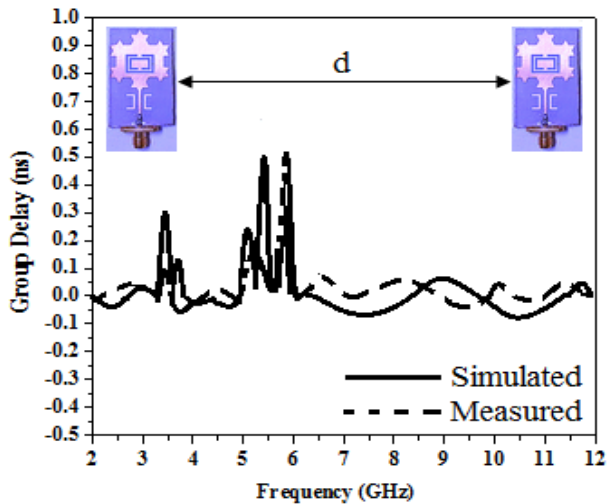


Figure 20. Time Domain analysis of proposed antenna.

4 Conclusion

The antenna we have designed and investigated here, is an UWB antenna with quadruple band notches. A fiberglass composite laminate G-10 fabric has been used as the substrate material, which makes it wearable. Complementary Split Ring Resonating Structures have been introduced at the centre of the radiator to generate band notches for the 03.5/05.2 GHz WiMAX/WLAN bands. Two ‘C-shaped’ parasitic structures have been placed by both sides of the feed line to generate a notched band for 05.5 GHz WiMAX band. Two ‘L-shaped’ open-ended slits have been introduced in the ground plane to produce a notch at 05.8 GHz for bypassing the WLAN band. The proposed fractal monopole antenna shows UWB response from 02.7 – 11.5 GHz excepting the four notched bands. Compactness, high durability, minimal moisture absorption, high resistance to chemicals along with multiple frequency eliminating technique account for the novelty of the proposed structure.

5 References

1. FCC Report and Order on Ultra Wideband Technology, Federal Commun. Commission, Washington, DC, USA, 2002.
2. Gao P, Xiong L, Dai J, He S and Zheng Y, Compact Printed Wide-Slot UWB Antenna With 3.5/5.5-GHz Dual Band-Notched Characteristics, *IEEE Antennas and Wireless Propagation Letters* 12: 983–86, 2013
3. Shuai C, Wang G and Zhou C, A novel compact ultra wideband antenna having dual frequency band-notched function. *IEEE International Conference on Microwave and Millimeter Wave Technology*, Beijing 710–12, 2016
4. Li Y, Yang X, Liu C, and Jiang T, Compact CPW-fed ultra-wideband antenna with dual band-notched characteristics, *IET Electronics Letters* 46: 967–68, 2010
5. Zhou Z, Li L, and Hong J, Compact UWB printed monopole antenna with dual narrow band notches for WiMAX/WLAN bands, *IET Electronics Letters* 47: 1111–12, 2011
6. Taheri M, Hassani H, and Mohammad S, UWB Printed Slot Antenna With Bluetooth and Dual Notch Bands, *IEEE Antennas and Wireless Propagation Letters* 10: 255–58 2011
7. Li L, Zhou Z, Hong J, and Wang B, Compact dual-band-notched UWB planar monopole antenna with modified SRR. *IET Electronics Letters* 47: 950–51 2011
8. Wang Z, Liu J, Yin Y, Triple band-notched UWB antenna using novel asymmetrical resonators. *AEU – Int J Electron Commun.* 70: 1630–36 2016
9. Wang Q, Zhang Y, Design of a Compact UWB Antenna with Triple Band-Notched Characteristics. *International Journal of Antennas and Propagation.* vol. 2014, Article ID 892765, 9 pages, 2014
10. Wu L, Xia Y, Cao X, Compact Quad Band-Notched Monopole Antenna for UWB Systems *Wireless Pers. Commun.* 95: 3617 2017
11. Koch HV, *Archive for Mathematics, Astronomy and Physics / Issued by K. Svenska Vetenskapsakademien* v.1 1903-1904
12. Naghshvarian M, Novel wideband planar fractal monopole antenna. *IEEE Transactions on Antennas and Propagation* 56: 3844-3849 2008